ISSN 1063-7834, Physics of the Solid State, 2010, Vol. 52, No. 10, pp. 2044–2057. © Pleiades Publishing, Ltd., 2010.
Original Russian Text © Yu.M. Baĭkov, 2010, published in Fizika Tverdogo Tela, 2010, Vol. 52, No. 10, pp. 1908–1920.

SEMICONDUCTORS AND DIELECTRICS

# Self-Diffusion of Lithium, Hydrogen, and Oxygen Ions in Crystalline Lithium Hydroxide

**Yu. M. Baĭkov**

*Ioffe Physical-Technical Institute, Russian Academy of Sciences, Politekhnicheskaya ul. 26, St. Petersburg, 194021 Russia*
*e-mail: baikov.solid@mail.ioffe.ru*

Received December 28, 2009; in final form, February 28, 2010

**Abstract**—The self-diffusion coefficients of ions of the three chemical elements forming lithium hydroxide have been determined by the crystal–crystal and crystal–gas isotope exchange method in the temperature range 500–720 K. Crystal samples with different isotope compositions have been grown by the Bridgman method from melts. The melting temperature is 743 ± 2 K. Original methods have been developed for high-precision measurements of the isotope ratios of all three elements, i.e., lithium ($^6$Li/$^7$Li), hydrogen (H/D), and oxygen ($^{16}$O/$^{18}$O), and their changes after diffusion annealings with the use of the same sample. The self-diffusion coefficients of lithium and hydrogen ions differ but by a factor of no more than 3–5; however, their values exceed those for oxygen by several orders of magnitude. In particular, at 670 K, they are equal to $6.0 \times 10^{-9}$, $3.2 \times 10^{-9}$, and $2.0 \times 10^{-12}$ cm$^2$ s$^{-1}$ for hydrogen, lithium, and oxygen, respectively. In the range 680–720 K, the self-diffusion coefficients of hydrogen and lithium increase sharply with increasing temperature to approximately $10^{-6}$ cm$^2$ s$^{-1}$. A probable mechanism of migration of protons and lithium ions in LiOH and the role played in this process by the oxygen ions with a lower mobility have been discussed.

**DOI:** 10.1134/S1063783410100070

## 1. INTRODUCTION

### *1.1. Metal Hydroxides: Basic Studies*

Lithium hydroxide LiOH belongs to a broad class of metal hydroxides, which have formally two structure-forming ions, a metal cation and a complex anion $OH^-$, i.e., the hydroxide ion. The specific features observed in the behavior of the latter in the crystal lattice can be traced to the presence of the proton. Moreover, the electronic and internal atomic–ionic structures of the hydroxide ion defy treatment within the same approach, which in the simplest form can be conceived of as a kind of competition among the states $O^{2-}H^+$, $O^-H^0$, and $O^0H^-$ (see, e.g., [1, 2]). While the hydroxide ion is not larger in size than the oxygen ion [2, 3], it nevertheless is a strong dipole because of the presence of the proton, which accounts for a significant contribution of orientation effects to the physical and chemical properties of solid hydroxides (see, e.g., [4–6]). In addition, the tiny nuclear-scale size of the proton confers to the hydroxide ion the capacity of forming the hydrogen bond, a truly unique type of chemical bonding [4, 7]. The O–H bonding plays a significant part in forming the conditions favoring protonic conduction, which in itself is a remarkable phenomenon among the processes involved in charge and mass transport in condensed media [3]. While lithium hydroxide as a "carrier" of hydroxide ions should be formally classed among alkali metal hydroxides, in actual fact, it occupies an intermediate position between the thermally stable alkali and other hydroxides, which decompose at temperatures substantially below their melting points.

### *1.2. Solid Hydroxides of Alkali Metals as Ionic Conductors*

When 40 years ago, development of electrochemical devices for the conversion and storage of energy exhibited explosive growth, a search for and/or refinement of both conductors with a high ionic conductivity (electrolytes) and the associated electrode materials became of prime importance. It is at that time that interest in the ionic conduction of the hydroxides of alkali metals has become evident. Interestingly, LiOH was considered as a possible $Li^+$ conductor (see [8] and the review in [9]), with the other members of the group, from NaOH to RbOH, assigned to possible protonic conductors [10–16]. In actual fact, originally (in the 1970s–1980s) protonic conduction of alkali hydroxides was assumed rather than proved. A serious argument for the high mobility of protons in these materials was provided by the investigation of proton self-diffusion by the isotope exchange methods in NaOH and KOH [17], and by the proton magnetic resonance approach for NaOH through RbOH [15, 16] conducted in the 1980s–1990s. The close relation between the phenomena of diffusion and electrical

conduction is well known, and the results amassed in their investigation provide mutually complementary contributions to models of ion migration. Studies of both conduction and (self)-diffusion and comparison of the findings reported by different researchers revealed that underestimation of the chemical activity of alkali hydroxides with respect to water vapor and carbon dioxide may result in the grain boundaries in polycrystalline alkali hydroxides becoming carriers of phases of a different chemical composition, more specifically, of crystal hydrate and/or carbonate species [10, 11, 15, 16, 18]. It would seem that this difficulty could be side-stepped by performing experiments on single crystals or polycrystalline samples containing large enough single-crystal regions, but preparation of high-quality samples appropriate for macroscopic diffusion measurements turned out anything but an easy problem. The only successful attempt was undertaken by El'kin [14] (Ioffe Physical-Technical Institute of the Russian Academy of Sciences, St. Petersburg), when special conditions were provided for the investigation of proton diffusion and the isotope effect in proton conduction in the high-temperature NaOH phase (568–585 K), in which a polycrystalline sample prepared by crystallization from melt and containing single-crystal regions 5–6 mm in size could be kept for three months with the temperature maintained within the above interval.

### *1.3. Physical and Chemical Properties of Solid Lithium Hydroxide*

The crystal structure of LiOH has space group $D_{4h}^7$, it is layered, *B*-10 type, and fairly loose. The latter can be seen from a comparison of the densities of lithium hydroxide and fluoride (1.43 and 2.23 g/cm$^3$, respectively), whose anions, $OH^-$ and $F^-$, are practically of the same size and differ in mass by ~10% only. The existence of polymorphic transformations in LiOH at normal pressure has been a matter of debate for the recent 50 years [18–20]. At the same time, the room-temperature phase transition characteristic of the other alkali hydroxides was observed to occur in LiOH at a pressure of several kilobars [20].

We may add that at an air humidity under laboratory conditions of ~20–30%, LiOH practically does not dehydrate up to 850 K, which is ~100 K above the melting point.

A pioneering investigation of ion self-diffusion in crystalline solid LiOH was carried out in 1974 at the Laboratory of physicochemical studies of isotopes, Ioffe Physical-Technical Institute, after one had succeeded in preparing crystalline samples meeting the requirements of traditional techniques accepted in diffusion research. A short communication was published on the self-diffusion coefficients of the $Li^+$ and $H^+$ ions [21]. In 1977, a publication [22] reported a low conductivity of solid LiOH, but identification of the current carriers (including electronic) was not more than tentative. NMR measurements of the mobility of $Li^+$ and $H^+$ in LiOH performed in 1978 were interpreted as evidence for the motion in the lattice of lithium ions rather than of protons [23]. Later (in 1987) [24], a comparison was performed of the electrical conductivities of LiOH derived from experiments [23] and calculated from the Nernst–Einstein relation based on refined data [21]. The question of the nature of the ionic current carriers did not, however, receive a convincing answer.

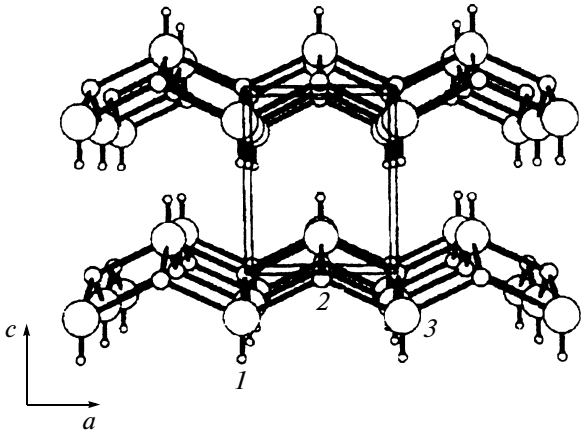


**Fig. 1.** LiOH structure under normal conditions in the form convenient for discussing the ion migration paths: (*1*) protons, (*2*) lithium ions, and (*3*) oxygen ions.

The layered LiOH structure can be illustrated by quasi-two-dimensional trilayer stacks, with the lithium ion layer sandwiched between two layers of hydroxide ions in each of them. The O–H bonds are directed outwards perpendicular to the stack plane. In the structure, one can see channels surrounded by proton-containing oxygen-ion orbitals and lithium ions (Fig. 1). A question naturally arises as to how such natural channels can affect the mobility of not only protons but of the lithium and oxygen ions as well. To unravel some details in the ion transport mechanism, it appeared essential to study on the same samples self-diffusion of ions of all the three elements making up LiOH, a problem that became the major goal of the present investigation. In the course of the experiments two additional problems bearing on the self-diffusion of protons and oxygen ions in LiOH have emerged. First, one had to ascertain the observation of oxygen ions having allegedly a lower mobility at 550–650 K than that of the hydrogen and lithium ions. Second, one had to study in more detail and confirm the anomalous growth with temperature of the hydrogen self-

diffusion rate in the 650–720-K region. We chose the isotope technique to probe the above two problems.

### *1.4. Isotope Exchange as a Method for Investigating (Self-)Diffusion*

Isotope exchange is a method traditionally employed in self-diffusion studies that had proved its efficiency. Experimental realization of the subject of the investigation can be tentatively divided in two groups, actually homophase and clearly heterophase ones. In the first case, one studies redistribution of the isotope of the chemical element of interest between two solid-phase samples of the same chemical, but different isotope composition, for instance, between the $^6$LiOH and $^7$LiOH crystals. The heterophase approach to studying the isotope exchange assumes investigation of the redistribution of the isotope of the chemical element under study between two samples differing not only in the isotope composition, but in the chemical and phase state as well; this could be, for instance, deuterium–protium exchange between crystalline LiOH and gaseous $D_2$. The present experiments used both the homophase realization (crystal–crystal exchange) and the heterophase approach based on the gas (hydrogen or oxygen)–crystal exchange. Being different, the techniques employed in these two versions are described separately below. At the same time, the original, isotopically different materials were prepared by the same scenario.

The main experimental parameter derived from a set of primary data in our experiments is the extent of isotope exchange $F$ at the given instant of time in each sample

$$F = \{C(t) - C(t = 0)\}/\{C(\text{eq}) - C(t = 0)\}, \quad (1)$$

where $C$ is the atomic fraction of the isotope under study, $t$ is the time from the beginning of diffusion annealing or the gas–crystal contact, and $C$(eq) is the atomic fraction of the observed isotope at equilibrium. The point is that it is not only the absolute content of an isotope that is of interest in the subsequent data treatment but the variation in this content with respect to its original value in the same sample. And it is the accuracy with which these changes are measured that is the decisive factor for the accuracy of the subsequent calculation of the (self-)diffusion coefficients and of the rates of isotope exchange reactions at the gas–crystal interface.

## 2. EXPERIMENTAL TECHNIQUE

### *2.1. Preparation of the Original Materials with Different Isotope Compositions*

The characteristics of diffusion and ionic conductivity in a solid depend substantially both on the impurities whose concentration not always can be monitored, and, not infrequently, on the texture of the material, if single crystals cannot be grown. To reduce the adverse effects of such factors on the reproducibility of results, it appeared necessary to perform both the synthesis of the starting materials and growth of lithium hydroxide crystals from them in the same conditions and by the same techniques, irrespective of the isotope compositions of the three elements.

The starting materials were isotopically different forms of liquid water and metallic lithium. Synthesis of lithium hydroxide through direct interaction of water with the metal was excluded because of the course of this reaction being difficult to monitor, and of the amounts of metallic $^6$Li and heavy-oxygen water $H_2{}^{18}O$ having been limited. We have therefore developed an ingenious method of synthesis through interaction of finely dispersed lithium hydride powder with water vapor at room temperature. The kinetics of this reaction had been studied earlier at the Ioffe Physical-Technical Institute [25].

We are omitting here the details of synthesis of lithium hydroxide used in the present study. We are stressing, however, an extremely important point, namely, that most of the procedures described here were performed in an atmosphere of an inert gas (nitrogen, argon) purified thoroughly from carbon dioxide and dried. Unless otherwise specified, we shall assume these conditions to remain unchanged and drop mentioning it.

The starting hydrogen- and oxygen-containing materials were (a) water of natural isotope abundance in hydrogen and oxygen, (b) water enriched in deuterium to 24.68 at % by mixing it with commercial "heavy" water having natural oxygen isotope composition, (c) water enriched in the $^{18}$O oxygen isotope to 58 at % and deuterium content of not over 0.1 at %.

All the three types of water passed three stages of distillation and had room-temperature conductivity not over $10^{-5}$ S cm$^{-1}$.

Gaseous hydrogen required for the synthesis of lithium hydroxide and isotope-exchange experiments was a mixture of $H_2$ and $D_2$ prepared electrolytically, followed by drying and removal of traces of oxygen.

The isotope composition of the starting metallic lithium was 7.52 at % $^6$Li and 90.88 at % $^7$Li. Chemical analysis of the starting samples did not reveal the presence of impurities of over 0.01 wt %, which was corroborated by spectral analysis of the hydroxide samples prepared subsequently.

Four lots of lithium hydroxide powder differing in the isotope composition were prepared. The precise values of the isotope composition of these materials

prepared for the subsequent experiments are listed in Table 1. Also shown is their notation accepted in the text below which uses either letters *A*, *B*, *X*, *Y* or formulas of the type $^{m}Li^{n}OH$ or $^{m}Li^{n}OD$, where $m = 6$ or 7, and $n = 16$ or 18. The formula LiOH is used below wherever specification of the isotope composition is not essential.

### *2.2. Crystalline Samples*

We prepared for experiments lithium hydroxide crystals of four types, with the isotope compositions of lithium, hydrogen, and oxygen specified in Table 1. The growth conditions refined on type *A* crystals were accepted for the other crystals as well. To grow LiOH crystals by the Bridgman technique, a powder sample was placed in sealed Armco iron ampoules. The temperature at the top of the furnace was 850 K. The temperature gradient in the furnace in the crystallization zone was 15 K cm$^{-1}$. The velocity of ampoule descent was 5 mm h$^{-1}$. On completion of the synthesis, the ampoule shell was removed mechanically. The diameter of the cylindrical samples thus obtained was 1.2 ± 0.1 cm. The single-crystal regions measured about 5 × 5 × 5 mm. The melting point of the crystals with natural isotope abundance of the three elements determined by differential scanning calorimetry was found to be 743 ± 2 K.

The grown crystals were divided into two groups.

Visual inspection with a microscope identified a group of well-crystallized samples without cracks and chipping. It was used in the crystal–crystal experiments. The pairs of samples intended for diffusion studies were cut from the starting specimens of this group perpendicular to the cylinder axes. The lengths of these samples are specified in columns 3, 4 of Table 2 and columns 5, 6 of Table 3.

Crystals of the second group were intended for investigation of the crystal–gas isotope exchange. The choice of samples for these experiments was determined by the fairly broad ranges not only of the expected diffusion coefficients (from $10^{-15}$ to $10^{-6}$ cm$^{-2}$ s$^{-1}$) but of the rates of hydrogen or oxygen exchange at the phase boundary (from $10^{-13}$ to $10^{-9}$ mol cm$^{-2}$ s$^{-1}$). For the diffusion experiments to be methodologically irreproachable, one had to work with LiOH samples with different specific surfaces. The choice for starting materials of grown crystals with their subsequent transformation into finely powdered crystalline or ball-shaped, small diameter samples was dictated by the wish to run all the experiments planned in the study on materials of the same technological history. The specific surface area was determined, depending on the form of the material, either geometrically or by mesh analysis, and/or again by krypton adsorption.

**Table 1.** Notation of isotopically different starting materials (lithium hydroxide powders)

| Notation | Lithium, at % | Oxygen, at % | Hydrogen, at % | Compound |
|---|---|---|---|---|
| *A* | 7.52 | 0.2* | 0.02* | $^{7}Li^{16}OH$ |
| *B* | 90.88 | 0.2* | 24.68 | $^{6}Li^{16}OD$ |
| *X* | 7.52 | 18.2 | 0.02* | $^{6}Li^{18}OD$ |
| *Y* | 7.52 | 18.2 | 0.02* | $^{7}Li^{18}OH$ |

* The values of the natural isotope abundance of hydrogen and oxygen in the table are rounded off, and the true values are equal to 0.016 and 0.202 at %, respectively.

### *2.3. Crystal–Crystal Isotope Exchange*

**2.3.1. Experimental technique.** The end faces of samples with different isotope compositions were ground, pressed with a weight of 0.5 kg, and placed in the diffusion anneal furnace in vacuum or thoroughly dried argon (with the dew point below liquid nitrogen boiling temperature). The diffusion anneal time was varied depending on the temperature, from 30 to 780 h, i.e., from one day to one month. The temperature creep in an experiment did not exceed ±0.5 K for "fast" anneals and ±1.5 K for experiments lasting more than 200 h. Figure 2 specifies isotopically different sample pairs selected for annealing at a set of temperatures. The anneal time is given in column 11 of Table 2 and column 12 of Table 3. Following the diffusion anneal, the samples were separated mechanically along the plane of contact and stored in separate ampoules up to the time of the isotope analysis.

**2.3.2. Isotope analysis of samples in the crystal–crystal experiments.** The specific physical-chemical properties of LiOH and some extraneous factors, such as the cost of the materials (the $^{6}Li$ and $^{18}O$ isotopes), determined development of a special approach to the isotope analysis of all the three elements making up LiOH in the same sample.

The lithium and hydrogen isotope compositions in samples of the *A* and *B* types (Table 2), i.e., materials

| | | | | |
|---|---|---|---|---|
| 573, 633, 666, 673, 693, 713 K | 598 K | 655, 713 K | 656, 670 678, 684, 687, 696 K | 598, 655, 713 K |
| $^{6}$**Li**$^{16}$**OD** (*B*) | $^{6}$**Li**$^{18}$**OD** (*X*) | $^{6}$**Li**$^{16}$**OD** (*B*) | **HD** | $^{16}$**O**$^{18}$**O** |
| $^{7}$**Li**$^{16}$**OH** (*A*) | $^{7}$**Li**$^{16}$**OH** (*A*) | $^{7}$**Li**$^{18}$**OH** (*Y*) | Li**O**H | Li$^{16}$**OH** |

**Fig. 2.** Isotopically different crystal–crystal or crystal–gas pairs studied in contact. Shown in bold are the ions whose isotopes were studied in the exchange experiment. The temperatures at which these pairs were studied are indicated.

**Table 2.** Experimental conditions and initial data needed for determining the self-diffusion coefficients of lithium and hydrogen in LiOH by the crystal–crystal isotope exchange method

| No. | $T$, K | Ion diffusing into the sample | Sample length, cm | | Theoretical shift, at % Y | Observed shift, at % | $F$(Li) | $\Delta F$(Li) | $F$(H) | $\Delta F$(H), $10^6$ s | Time |
|---|---|---|---|---|---|---|---|---|---|---|---|
| | 1 | 2 | 3 | 4 | 5 | 6 | 7 | 8 | 9 | 10 | 11 |
| 1 | 573 | $^6$Li($C$) ⟶ $^7$LiOH($A$) | | 1.12 | 7.52 ⟶ 43.7 | −0.19 | 0.006 | 0.003 | | | 2.18 |
| 2 | | $^7$Li($A$) ⟶ LiOD($B$) | 0.86 | | 90.88 ⟶ 43.7 | 0.26 | 0.005 | 0.003 | | | |
| 3 | | D($B$) ⟶ $^7$LiOH($A$) | | 1.12 | 0.02 ⟶ 10.72 | *0.31* | | | 0.029 | 0.002 | |
| 4 | | H($A$) ⟶ $^6$LiOD($B$) | 0.86 | | 24.68 ⟶ 10.72 | *−0.45* | | | 0.032 | 0.004 | |
| 5 | 598 | $^6$Li($X$) ⟶ $^7$LiOH($A$) | | 1.3 | 7.52 ⟶ 75.25 | 7.38 | 0.107 | 0.008 | | | 3.1 |
| 6 | +O | $^7$Li($A$) ⟶ LiOD($X$) | 0.3 | | 90.88 ⟶ 75.25 | −1.7 | 0.109 | 0.008 | | | |
| 7 | | D($X$) ⟶ $^6$LiOH($A$) | | 1.3 | 0.02 ⟶ 20.06 | *1.16* | | | 0.058 | 0.002 | |
| 8 | | H($A$) ⟶ $^6$LiOD($X$) | 0.3 | | 24.68 ⟶ 20.06 | −0.27 | | | 0.060 | 0.004 | |
| 9 | 633 | $^6$Li ⟶ $^7$LiOH($A$) | | 1.5 | 7.52 ⟶ 39.8 | 1.93 | 0.06 | 0.01 | | | 2.63 |
| 10 | | $^7$Li ⟶ $^6$LiOD($B$) | 0.95 | | 90.88 ⟶ 39.8 | −3.17 | 0.062 | 0.008 | | | |
| 11 | | D($B$) ⟶ $^7$LiOH($A$) | | 1.5 | 0.02 ⟶ 9.57 | *0.28* | | | 0.029 | 0.005 | |
| 12 | | H($A$) ⟶ $^6$LiOD($B$) | 0.95 | | 24.68 ⟶ 9.57 | *−0.48* | | | 0.032 | 0.045 | |
| 13 | 655 | $^6$Li($B$) ⟶ $^7$LiOH($Y$) | 0.3 | | 7.52 ⟶ 15.63 | 2.48 | 0.306 | 0.008 | | | 2.63 |
| 14 | +O | $^7$Li($Y$) ⟶ $^6$LiOD($B$) | | 1.3 | 90.88 ⟶ 15.63 | −1.38 | 0.298 | 0.008 | | | |
| 15 | | D($B$) ⟶ $^7$LiOH($Y$) | 0.3 | | 0.02 ⟶ 20.06 | *6.93* | | | 0.384 | 0.009 | |
| 16 | | H($Y$) ⟶ $^6$LiOD($B$) | | 1.3 | 24.68 ⟶ 20.06 | *−1.73* | | | 0.374 | 0.009 | |
| 17 | 666 | $^6$Li ⟶ $^7$LiOH($A$) | | 1.06 | 7.52 ⟶ 49.8 | 3.57 | 0.084 | 0.008 | | | 2.76 |
| 18 | | $^7$Li ⟶ $^6$LiOD($B$) | 1.03 | | 90.88 ⟶ 49.8 | −3.63 | 0.088 | 0.008 | | | |
| 19 | | D($B$) ⟶ $^7$LiOH($A$) | | 1.06 | 0.02 ⟶ 12.17 | *1.29* | | | 0.106 | 0.012 | |
| 20 | | H($A$) ⟶ $^6$LiOD($B$) | 1.03 | | 24.68 ⟶ 12.17 | *−1.45* | | | 0.116 | 0.009 | |
| 21 | 673 | $^6$Li ⟶ $^7$LiOH($A$) | | 1.48 | 7.52 ⟶ 49.2 | 2.22 | 0.050 | 0.006 | | | 1.75 |
| 22 | | $^6$Li ⟶ $^6$LiOD($B$) | 1.48 | | 90.88 ⟶ 49.2 | −2.06 | 0.053 | 0.006 | | | |
| 23 | | D($B$) ⟶ $^7$LiOH($A$) | | 1.48 | 0.02 ⟶ 12.34 | *0.99* | | | 0.080 | 0.002 | |
| 24 | | H($A$) ⟶ $^6$LiOD($B$) | 1.48 | | 24.68 ⟶ 12.34 | *−1.20* | | | 0.084 | 0.002 | |
| 25 | 693 | $^6$Li ⟶ $^7$LiOH($A$) | | 1.625 | 7.52 ⟶ 54.64 | −16.7 | 0.28 | 0.04 | | | 0.295 |
| 26 | | $^7$Li ⟶ $^6$LiOD($B$) | 1.25 | | 90.88 ⟶ 54.64 | 10.25 | 0.35 | 0.06 | | | |
| 27 | | D($B$) ⟶ $^7$LiOH($A$) | | 1.625 | 0.02 ⟶ 10.74 | *4.32* | | | 0.403 | 0.001 | |
| 28 | | H($A$) ⟶ $^6$LiOD($B$) | 1.25 | | 24.68 ⟶ 10.74 | *−5.86* | | | 0.042 | 0.002 | |
| 29 | 713 | $^6$Li ⟶ $^7$LiOH($A$) | | 1.45 | 7.52 ⟶ 49.2 | −8.29 | 0.199 | 0.008 | | | 0.1 |
| 30 | | $^7$Li ⟶ $^6$LiOD($B$) | 1.45 | | 90.88 ⟶ 49.2 | 8.48 | 0.203 | 0.006 | | | |
| 31 | | D($B$) ⟶ $^7$LiOH($A$) | | 1.45 | 0.02 ⟶ 12.34 | *2.58* | | | 0.21 | 0.002 | |
| 32 | | H($A$) ⟶ $^6$LiOD($B$) | 1.45 | | 24.68 ⟶ 12.34 | *−3.15* | | | −0.22 | 0.002 | |

with a natural oxygen abundance ($^{18}$O abundance ≈ 0.2 at %), was determined densitometrically by the flotation technique developed at the laboratory of physicochemical studies of isotopes (Ioffe Physical-Technical Institute). This method provides particularly high precision when used to compare isotope compositions of two or more samples (for instance, of a sample in the as-prepared and diffusion-annealed states). The chemical procedures involved in transformation of lithium hydroxide with a natural oxygen isotope abundance into samples intended for determination of the isotope composition of lithium and hydrogen were started with crushing the starting materials in an agate mortar. A calibrated volume of the powder thus obtained was brought in contact with carbon dioxide at 420–500 K, and the water forming in the process was collected in a cooled quartz test tube. Special calibrated quartz floats were employed to compare the

**Table 3.** Experimental conditions and initial data for the determination of the oxygen mobility in LiOH

| No. | $T$, K | Method | Theoretically possible shift $^{18}O$, at % | Measured shift $^{18}O$, at % | Experimental conditions | | | | | $F$ | $\Delta F$ | Time, $10^6$ |
|---|---|---|---|---|---|---|---|---|---|---|---|---|
| | | | | | sample length, cm | | $S$, $cm^{-1}$ | λ | $P$, kPa | | | |
| | 1 | 2 | 3 | 4 | 5 | 6 | 7 | 8 | 9 | 10 | 11 | 12 |
| 1 | 598 | Cr–Cr | 18 ⟶ 14.66 | <0.01 | | $X \sim 1.3$ | | | | <0.003 | 0.01 | 3.1 |
| 2 | | The same | 0.2 ⟶ 14.66 | <0.02 | $A \sim 0.3$ | | | | | <0.0016 | 0.01 | 3.1 |
| 3 | | Cr–Gas | 0.2 ⟶ 28 | 0.2 ⟶ 0.4 | | | 420 | 1 | 7 | 0.011 | 0.001 | 8.64 |
| 4 | | The same | 0.2 ⟶ 28 | 0.2 ⟶ 0.75 | | | 420 | 1 | 7 | 0.034 | 0.002 | 27 |
| 5 | 655 | Cr–Cr | 18 ⟶ 3.5 | –0.08 | $Y \sim 0.3$ | | | | | 0.006 | 0.002 | 2.63 |
| 6 | | The same | 0.2 ⟶ 3.5 | 0.01 | | $B \sim 1.3$ | | | | 0.003 | 0.002 | 2.63 |
| 7 | | Cr–Gas | 0.2 ⟶ 28 | 0.2 ⟶ 0.31 | | | 30 | 1 | 7 | 0.004 | 0.002 | 0.8 |
| 8 | | The same | 0.2 ⟶ 28 | 0.2 ⟶ 0.78 | | | 30 | 1 | 7 | 0.028 | 0.001 | 8.7 |
| 9 | | ″ | 0.2 ⟶ 28 | 0.2 ⟶ 2 | | | 30 | 1 | 7 | 0.07 | 0.005 | 27 |
| 10 | 713 | Cr–Cr | 18 ⟶ 15.4 | –0.06 | $Y \sim 1.45$ | | | | | 0.02 | 0.003 | 1.4 |
| 11 | | The same | 0.2 ⟶ 15.4 | 0.36 | | $B \sim 0.25$ | | | | 0.024 | 0.002 | 1.4 |
| 12 | | Cr–Gas | 0.2 ⟶ 5.47 | 0.2 ⟶ 0.6 | | | 52 | 10 | 70 | 0.112 | 0.01 | 0.86 |
| 13 | | The same | 0.2 ⟶ 5.47 | 0.2 ⟶ 2.25 | | | 52 | 10 | 70 | 0.41 | 0.05 | 4.24 |
| 14 | | ″ | 0.2 ⟶ 5.47 | 0.2 ⟶ 3.7 | | | 52 | 10 | 70 | 0.68 | 0.05 | 8.64 |

Note: (Cr–Cr) Crystal–crystal, (Cr–Gas) crystal–gas.

densities of this water and of the starting water (with a natural isotope composition or containing 24.68 at % deuterium). The lithium carbonate produced in the reaction was converted to fluoride. The density of the LiF single crystals shaped as hemispheres, 3–4 mm in diameter each, prepared by the Kyropoulos method, was compared with that of LiF single crystals grown from the starting materials. The differences in flotation temperatures of 0.02–0.04°C could be accurately measured with Beckman thermometers as well as derived from the difference in equilibrium temperatures between two crystals or between a crystal and a calibration float placed in the same liquid, by analyzing the behavior of the float motion rates with temperature. These values can be translated into the variations in the hydrogen isotope composition by 0.01 at %, and of lithium, by 0.04 at %.

The shifts of the isotope composition of lithium and hydrogen from the starting figures in pairs of samples subjected to diffusion annealing are confronted with the results or densitometric analysis in column 6 of Table 2. For convenience, the variations in the isotope composition of lithium (in at % $^6Li$) are identified with straight font (rows 1, 2; 5, 6; 9, 10; 13, 14; 17, 18; 21, 22; 25, 26; 29, 30), and those of hydrogen (in at % D), with italics (rows 3, 4; 7, 8; 11, 12; 15, 16; 19, 20; 23, 24; 27, 28; 31, 32).

The isotope composition of both oxygen and hydrogen in samples containing "heavy" oxygen with the starting fraction of $^{18}O$ varying, depending on the actual goal of the experiment, from 58 at % down, was measured with a mass spectrometer. In this case, the sample was dehydrated in a closed volume with the temperature raised gradually to 850 K. The water vapor formed was collected in a test tube cooled with liquid nitrogen, thus ensuring practically total dehydration. After this, the test tube with water was connected through an adjustable valve to a quartz tube containing red-hot coal (900 K). The mixture of hydrogen, $H_{2-x}D_x$, and carbon dioxide, $C^{16}O_y{}^{18}O_{1-y}$, was analyzed with a mass spectrometer. The isotope composition of the gases was derived from the 2 : 3 : 4 peak ratio for hydrogen, and the 28 : 30 peak ratio for oxygen. The $Li_2O$ residue was converted to fluoride for the subsequent densitometric analysis. The data for oxygen can be found in cells at the crossing points of column 4 with rows 1, 2; 5, 6; and 10, 11 in Table 3. The data for hydrogen obtained by gas analysis are listed in column 6 of Table 2 (italics, rows 7, 8 and 15, 16). Column 1 of Table 2 for these experiments contains also, besides the temperature, a symbol +O, which denotes combined observation of diffusion of all the three elements.

The extents of exchange $F$ and the estimated error in their determination $\Delta F$, which takes into account

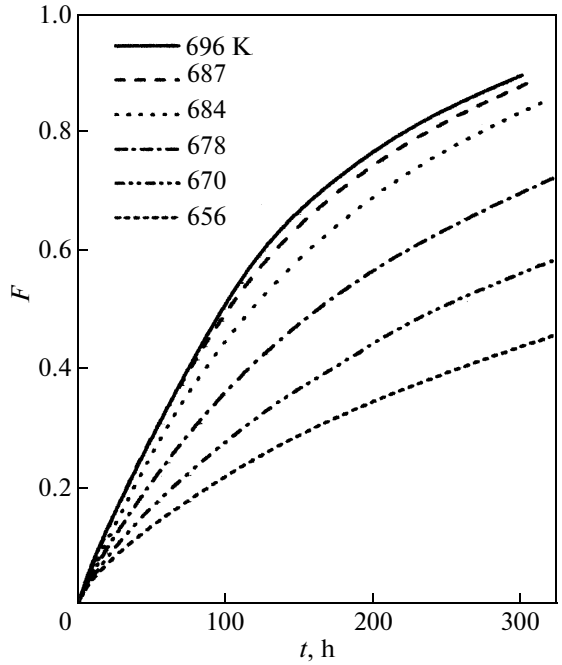


**Fig. 3.** Kinetics of deuterium–protium exchange between molecular hydrogen and lithium hydroxide plotted in the extent of exchange $F$–time $t$ coordinates at different temperatures.

not only the accuracy with which the isotope composition is measured but various experimental factors, are presented in Table 2 (columns 7–10) and Table 3 (columns 10, 11). The value of $C$(eq) required to derive the extent of exchange was determined by calculation with due account of the isotope composition of the starting samples (before annealing) and of the ratios of the numbers of atoms of the corresponding chemical element in these samples. In Table 2 (column 5) and Table 3 (column 3), the corresponding values of $C$(eq), for all samples in all the isotope pairs, are given to the right of the arrow, with the values of $C(t = 0)$ shown to the left of it.

### *2.4. Heterogeneous Isotope Exchange Solid LiOH–Gas ($H_2$ or $O_2$)*

**2.4.1. Organization of experiments and isotope analysis of the gas phase.** The gas–crystal isotope exchange was studied in quartz flasks of different calibrated capacities into which quartz boats with the required amount of the hydroxide, in the form of a powder or specially prepared samples, was placed. The gases were sampled through valves which connected with the mass spectrometer in different ways, depending on the experiment duration. The gas sampling conditions were chosen such that the variation in the gas pressure, i.e., of the number of atoms taking part in the isotope exchange, did not exceed 10–15%. The isotope analysis of the gas phase was run with mass spectrometers of various types calibrated against specially prepared $H_2$ and $D_2$ mixtures or a mixture of molecular oxygen of natural abundance with oxygen enriched in the "heavy" isotope, where the atomic fraction of $^{18}O$ was ~0.002 and 0.580, respectively. Our measurements suggest that the fraction of $^{17}O$, which was higher than its natural abundance, was not larger than 0.01. The gas–crystal pairs studied in the experiment are shown in Fig. 2 on the right.

**2.4.2. Hydrogen isotope exchange.** The gas–crystal isotope exchange was studied in the temperature interval 656–696 K, in which the hydrogen self-diffusion coefficient was found to undergo an anomalously strong variation, from $10^{-9}$ to $10^{-7}$ cm$^2$ s$^{-1}$. These values and estimates of the hydrogen exchange rate at the crystal–gas interface made from data available on homomolecular exchange suggested that the samples intended for measurement of the hydrogen self-diffusion should have a small specific surface area $S < 10$ cm$^{-1}$. The original crystal samples (see Subsection 2.2) were used to prepare ten samples ~240 mg in weight and about 0.17 cm$^3$ in volume each. For this purpose, a pellet 1.2 cm in diameter and 0.35 cm thick was cut in half, and sharp edges were carefully removed. The surface area of such a sample was ≈6 cm$^{-1}$. The isotope composition of such samples corresponded to type $A(^7LiOH)$ (Table 1). The original gas phase was molecular hydrogen with the isotope composition $H_{2-x}D_x$ at a pressure of ~20 kPa. The volume of each flask was ~550 cm$^3$. The ratio of the amounts of hydrogen atoms in the gas and in the solid phase under these conditions was $\lambda \sim 1$. The variation with time of the extent of hydrogen isotope exchange is shown graphically in Fig. 3. For the sake of convenience, the time is given in hours.

**2.4.3. Oxygen isotope exchange.** The isotope exchange in the molecular oxygen–crystal system (column 2, Table 3) was studied at the same three temperatures as chosen for the crystal–crystal experiments: 598, 655, and 713 K. The experimental conditions and raw data are listed in rows 3, 4; 7–9, 12–14 of Table 3; $S$ is the specific surface area, $\lambda$ is the ratio of the amounts of oxygen atoms in the gas and the solid phases, and $P$ is the gas pressure. The duration of an experiment, from start to the time of gas sampling, is given in column 12. The shifts of the $^{18}O$ fraction in the gas phase at the theoretically possible gas–crystal equilibrium and the values observed experimentally are listed in columns 3 and 4 of Table 3, accordingly. Columns 10, 11 specify the extent of exchange $F$ and possible errors $\Delta F$ of these values, with due allowance for various factors.

Figure 4 confronts data on the extent of oxygen isotope exchange reached in both scenarios of the isotope exchange, namely, gas–crystal (*1a–3a*) and crystal–crystal (*1b–3b*). The measurements were performed at 713 (*1a*, *1b*), 655 (*2a*, *2b*), and 598 K (*3a*, *3b*). A comparison of the values of $F(t)$ in Figs. 3 and 4 shows convincingly, even without invoking careful mathematical treatment, that the mobility of oxygen in LiOH is noticeably lower than that of hydrogen. Indeed, a 50% exchange of hydrogen is completed in ~400 h at 656 K and in 100 h at 696 K, while that of oxygen, even at 713 K, in as long as 1900 h only.

## 3. RESULTS AND DISCUSSION

### *3.1. Calculation of the Self-Diffusion Coefficients of LiOH Ions*

The technique used in the experimental data treatment in this study is usually called "the average isotope composition method", referred to below as "the average composition method" which is based on determination of the total number of isotope atoms of the chemical element of interest, which have transferred from one sample into the other in the course of diffusion anneal. This is realized by measuring after a preset time the changes in the average isotope composition of the crystalline or gaseous sample on the whole. This is the major difference of the "average composition method" from the sectioning approach [26]. In both cases, crystalline samples make it possible to obtain only one point in contact duration, because the isotope analysis methods employed here involve destruction of the samples. Analysis of both contacting solid samples offers actually two values of the diffusion coefficient for a given temperature. Analysis of the gas phase permits one to follow the process in time, provided the gas is stirred efficiently and a possibility is provided to sample a small part of the gas for an isotope analysis.

**3.1.1. Crystal–crystal isotope exchange.** The calculations included the loss of the sample contact layer resulting from saw cutting (layer width 0.1 mm), dividing it equally between the pair members

$$1 - F = \exp(-Z_g^2)/(\pi^{1/2}(Z_d - Z_g)) - \{(Z_d - Z_g\mathrm{erf}Z_g)/(Z_d - Z_g)\}, \quad (2)$$

where $Z_d = d/(4\mathcal{D}t)^{1/2}$, $Z_g = g/(4\mathcal{D}t)^{1/2}$, $\mathcal{D}$ is the diffusion coefficient, and $d$ and $g$ are the sample length and saw-cut half-width, accordingly. Actually, we selected the values of $\mathcal{D}$ for the corresponding ions based on the experimentally determined values of $F(t)$ and the dimensions of the samples used, which are given in Tables 2 and 3. The values of $\mathcal{D}$(Li), $\mathcal{D}$(H), and $\mathcal{D}$(O) obtained in both (crystal–crystal and gas–crystal) versions of the isotope exchange are presented for comparison in Table 4, and plotted vs. temperature in Fig. 5. Figure 5 specifies for each temperature two values obtained for each member of the diffusion pair, and their mean is listed in Table 4. Figure 5 confronts also for comparison the values of the hydrogen and oxygen diffusion coefficients measured in the crystal–gas experiments (see below).

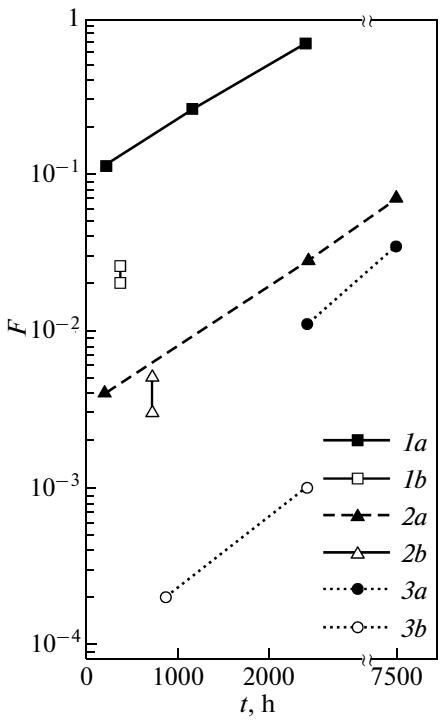


**Fig. 4.** Oxygen isotope exchange (*1a–3a*) between molecular oxygen and lithium hydroxide and (*1b–3b*) between two crystals with different $^{18}O$ contents. The temperatures of the experiments, K: (*1a*, *1b*) 713, (*2a*, *2b*) 655, and (*3a*, *3b*) 598. The lines are to guide the eye only.

**3.1.2. Crystal–gas isotope exchange.** The development of approaches to analysis of the gas–crystal isotope exchange $C_i(t)$ with the purpose of finding diffusion coefficients in the bulk of the solid phase ($\mathcal{D}$, $cm^2\ s^{-1}$) and of the rates of exchange through the contact surface ($I_0$, mol $cm^{-2}\ s^{-1}$), which dates back more than 60 years, stems from the need of planning an experiment and progress in computer applications [14, 26, 27]. Combining the nonlinear least-squares techniques with comparison of the shapes of experimental curves with model expectations, that is, relations derived from exact mathematical solutions, turned out an efficient approach to analysis of hydrogen isotope exchange. Because of the lack of a detailed set of experimental points within a broad enough range of $F$ and $t$ for the oxygen–hydroxide isotope exchange, we had to restrict ourselves to a conclusion which, while

**Table 4.** Self-diffusion coefficients of ions of lithium $\mathcal{D}$(Li), hydrogen $\mathcal{D}$(H), and oxygen $\mathcal{D}$(O) in crystalline lithium hydroxide; exchange rates at the contact surface with hydrogen $I_0$(H) and oxygen $I_0$(O) at a pressure of 7 kPa; and dimensionless parameters α characterizing the ratio of diffusion rates in the volume to those at the surface

| $T$, K | Method | $\mathcal{D}$(Li), $cm^2\ s^{-1}$ | $\mathcal{D}$(H), $cm^2\ s^{-1}$ | $\mathcal{D}$(O), $cm^2\ s^{-1}$ | α | $I_0$(H), $mol\ cm^{-2}\ s^{-1}$ | $I_0$(O), $mol\ cm^{-2}\ s^{-1}$ |
|---|---|---|---|---|---|---|---|
| 573 | Crystal–crystal | $8 \times 10^{-11}$ | $5 \times 10^{-11}$ | | | | |
| 598 | The same | $3.5 \times 10^{-10}$ | $1.5 \times 10^{-10}$ | $<1 \times 10^{-15}$ | | | |
| 633 | " | $1.5 \times 10^{-9}$ | $8 \times 10^{-10}$ | | | | |
| 655 | " | $2.5 \times 10^{-9}$ | $3.1 \times 10^{-9}$ | $\sim 4 \times 10^{-13}$ | | | |
| 666 | " | $3 \times 10^{-9}$ | $5.3 \times 10^{-9}$ | | | | |
| 673 | " | $3.5 \times 10^{-9}$ | $8.2 \times 10^{-9}$ | | | | |
| 693 | " | $5 \times 10^{-7}$ | $8.3 \times 10^{-7}$ | | | | |
| 713 | " | $7 \times 10^{-7}$ | $8.4 \times 10^{-7}$ | $1 \times 10^{-10}$ | | | |
| 598 | Gas–crystal | | | $1 \times 10^{-15}$ | 6.4 | | $1.6 \times 10^{-13}$ |
| 655 | The same | | | $4.5 \times 10^{-13}$ | 4.4 | | $3 \times 10^{-12}$ |
| 656 | " | | $3 \times 10^{-9}$ | | 6.3 | $6.8 \times 10^{-9}$ | |
| 670 | " | | $6 \times 10^{-9}$ | | 3.5 | $8.1 \times 10^{-9}$ | |
| 678 | " | | $1.3 \times 10^{-9}$ | | 1.98 | $8.9 \times 10^{-9}$ | |
| 680 | " | | $>6 \times 10^{-8}$ | | ~0.4 | $9.5 \times 10^{-9}$ | |
| 684 | " | | $>1 \times 10^{-7}$ | | <0.1 | $9.8 \times 10^{-9}$ | |
| 696 | " | | $>3 \times 10^{-7}$ | | <0.1 | $1.1 \times 10^{-8}$ | |
| 713 | " | | | $>4 \times 10^{-11}$ | <0.5 | | $1.8 \times 10^{-9}$ |

being reliable, is rather of a qualitative nature, namely, of the oxygen mobility in hydroxide being comparatively low.

The isotope exchange of hydrogen was studied within a narrow forty-degree interval 656–696 K in order to refine the behavior of hydrogen diffusion with temperature, which, judging from the crystal–crystal experiments, could be tentatively characterized by an activation energy of 5–7 eV (!). The choice of the gas–crystal system for solution of this problem was predicated by a number of factors, the most essential of them having been a wish to compare the hydrogen mobilities at different temperatures on samples as close in size and shape as possible.

The kinetic curves of heterogeneous isotope exchange may be considered as a sum of exponential terms, so that

$$1 - F = \Sigma A_i(a, q_i)\exp(-q_i^2 S^2 \mathcal{D} t), \qquad (3)$$

where $q_i = q_i(a)$ are positive roots of the equation $\tan q_i = q_i/((q_i^2/a) - 1)$. All expressions presented here relate to the specific case of our experiments, in which the ratio of the numbers of atoms of the observed element λ in the two phases is the same (λ = 1). The dimensionless quantity $a = I_0/\mathcal{D}NS$, where $N =$ 0.595 mol $cm^{-3}$ is the volume concentration of each of the chemical elements making up LiOH, and $S = 6\ cm^{-1}$ is the specific surface of our samples (see Subsection 2.4.2). Omitting here a tedious mathematical analysis of the behavior of the $F(t)$ curves for different values of the $a$ parameter, we stress the following points. The values $a < 0.5$ are observed typically when isotope exchange on the contact surface is the slowest stage. Also, the first nonzero root of the characteristic equation $q_1 \approx a^{1/2} \ll q_2$, and, therefore, the only term left in Eq. (3) is the exponential with the exponent $q_1^2 S^2 \mathcal{D} \approx aS^2\mathcal{D} = I_0 S/N$ and the prefactor $A_1 \approx 1$. By contrast, the values $a > 10$ turn out typically when the slowest stage is self-diffusion in the volume. Significantly, the ratio of the "neighboring" roots of the characteristic equation $q_{i+1}/q_i \approx \pi$. As a result, expansion (3) converges very poorly, but under certain conditions (see [27]) it can be folded into a function to produce in the $F$–$t^{1/2}$ coordinates a slowly varying curve convex to the ordinate axis. We note that, when plotted in these coordinates, the relations of the type $1 - F = \exp(-\gamma t)$ represent $S$-shaped curves symmetric with respect to the point with $F = 0.395$. In the intermediate case of gas–crystal isotope exchange kinetics, i.e., where $0.5 < a < 10$, one likewise observes an $S$-shaped curve, but it is noticeably nonsymmetric. This can be seen from Fig. 6 (the graph for 656 K). Plotted in the $\ln(1 - F)$–$t$ coordinates, these curves exhibit typically devia-

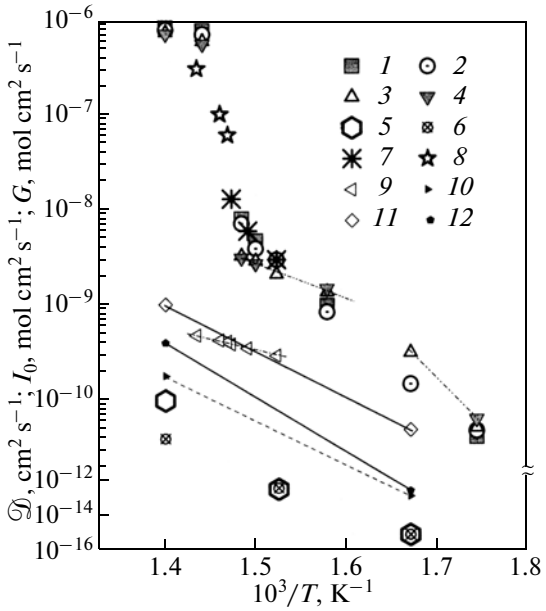


**Fig. 5.** Self-diffusion coefficients of (*1*, *2*) protons, (*3*, *4*) lithium ions, and (*5*, *6*) oxygen ions. For oxygen: (*5*) from crystal–crystal experiments and (*6*) from gas–crystal experiments (Table 4). At 713 K, point *6* indicates the lower limit of the oxygen diffusion coefficient $\mathcal{D}$(O). Pair points for lithium and hydrogen were obtained in crystal–crystal experiments after analysis of the isotope shifts in both samples. (*7*) Hydrogen diffusion coefficient $\mathcal{D}$(H) derived from fitting of the kinetic curves (see text). (*8*) Lower limit of $\mathcal{D}$(H) established in hydrogen–LiOH experiments. Dashed curves labeled by *9* and *10* represent the heteroexchange rates $I_0$ for hydrogen and oxygen, respectively. Continuous straight lines labeled by *11* and *12* correspond to the homoexchange rates obtained at a pressure of 7 kPa for hydrogen $G_3$ and oxygen $G_2$, respectively. For convenience, the values of $G_3$ are shown scaled down by a factor of 10.

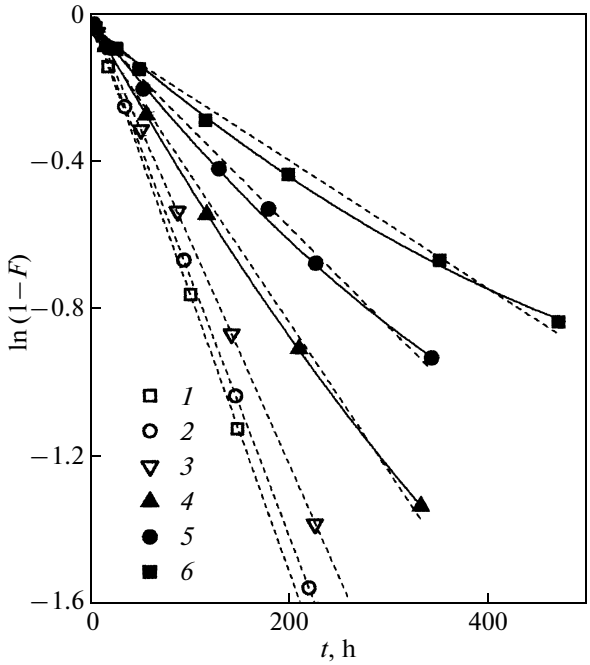


**Fig. 6.** Pronounced change in the shape of the kinetics curves visualizing deuterium–protium exchange between molecular hydrogen and lithium hydroxide observed in the temperature range 656–696 K. At (*1*) 696, (*2*) 684, and(*3*) 680 K, $\ln(1-F) = -\gamma t$, i.e., the isotope exchange at the contact surface is the slowest stage. At (*4*) 678, (*5*) 670, and (*6*) 656 K, the relation $\ln(1-F)$–$t$ deviates from a linear behavior, which is characteristic of diffusion-induced slowing-down of the exchange reaction.

tions from the linear course of the type seen in Fig. 7 for 656, 670, and 678 K. Such a curved pattern implies, in the language of mathematics, that expansion (3) contains more than one significant exponentials, whose number grows with increasing role of diffusion processes. The above considerations provided an additional basis for fitting of the curves for 656, 670, and 678 K; the values of $a$, $\mathcal{D}$, and $I_0$ are listed in Table 4. Different versions of fitting performed on three other curves revealed only one exponential. The latter implies that at temperatures of 689, 684, and 696 K one can obtain an estimate only for the lower limit of the hydrogen diffusion coefficient, which is specified in Table 4 together with the exact values of $I_0$ for the same temperatures obtained in the experiment. The variation in the hydrogen self-diffusion coefficients with temperature plotted in Fig. 5 provides supportive evidence for the anomalously fast, but regular growth of the hydrogen diffusion rate in LiOH in the interval 656–696 K.

The isotope exchange of oxygen was performed with the aim of estimating the diffusion coefficient of oxygen by a method different from the crystal–crystal exchange, and throughout the whole temperature range of 550–720 K. Indeed, in the crystal–crystal experiments the self-diffusion coefficient of oxygen ions was determined actually at 713 K only ($\sim 10^{-10}$ $cm^2\ s^{-1}$). But even at this temperature, the observed shift of the $^{18}O$ content in the gas was found to be 0.36 at %, which is only twice the $^{18}O$ content in oxygen of natural isotope abundance. Therefore, one could establish reliably, albeit not more than quantitatively, the slow exchange of the $^{16}O$ and $^{18}O$ isotopes between the crystals in contact. This could be assigned, however, to a variety of factors. Nevertheless, such a side reason as a "poor" mechanical contact between the crystals can be rejected basing on the substantially higher exchange rate in the same (!) hydrogen and lithium pairs (Table 2, 598 and 665 K). It is to estimate the chemical mobility of oxygen in surface hydroxide ions that the two types of oxygen isotope exchange, $O_2$ gas–LiOH powder, i.e., homomolecular equilibration (homoexchange, see Appendix) and heteroexchange, as described earlier for hydrogen, were conducted.

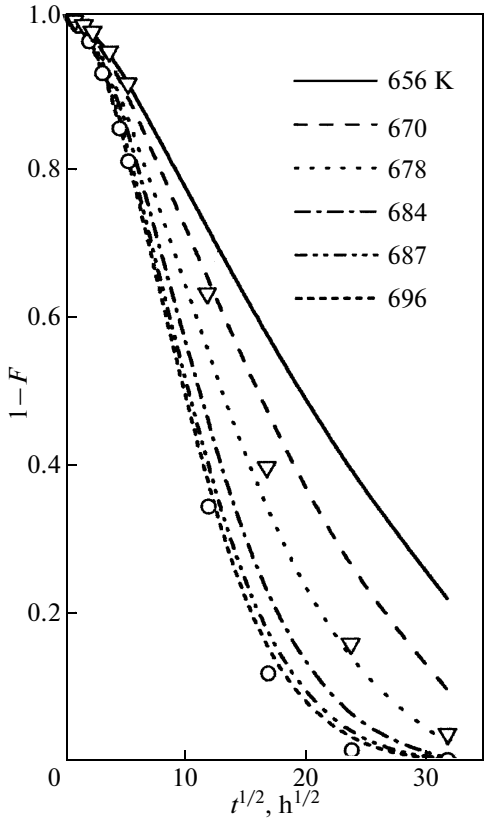


**Fig. 7.** Deuterium–protium exchange between molecular hydrogen and lithium hydroxide in the temperature range 656–696 K in the $(1 - F) - t^{1/2}$ coordinates that illustrates a change in the curve shape from symmetric *S*-shaped at 696 K (circles) to asymmetric at 656 K (triangles). This indicates a change in the contribution of diffusion-associated limitations to the isotope exchange rate (see text).

Examining Fig. 4, we see that while heteroexchange did not demonstrate very high extents of exchange, they are nevertheless larger than the figures realized in the crystal–crystal exchange; indeed, the points for heteroexchange (*1a–3a*) lie higher than those measured in homoexchange (*1b–3b*). By invoking the same approach as was used in the analysis of the isotope exchange of hydrogen (see above), we have succeeded in estimating self-diffusion of oxygen ions (Table 4), albeit with a noticeable scatter (Fig. 5). Nevertheless, it appears basically clear that for temperatures below 700 K the mobility of oxygen in LiOH is indeed slower than that of lithium and hydrogen (proton).

### *3.2. On the Mechanism of Migration of Lithium and Hydrogen Ions*

In discussing the mechanism underlying self-diffusion of the ions of lithium and hydrogen, which are more mobile than those of oxygen, we shall invoke the universally accepted concepts on the mobility of cations in compounds with substantially larger anions of the type of AgI and protons in oxygen-containing compounds of the type of $CsHSO_4$. Being basically disordered, the compounds presented here for the sake of illustration may be treated as ionic conductors. In AgI, this disorder originates from a large number of interstices surrounded by the large anions $I^-$ and accessible for the $Al^+$ ions. In $CsHSO_4$, the intrinsic disorder originates also from the large number of sites accessible for protons, but these are not the interstices but rather the orbitals of oxygen-containing ions. The simplest quasi-chemical equations can be developed in this context in the notation of Kröger–Vink as

$$\mathrm{Li}^x_{\mathrm{Li}} + V^x_i \Leftrightarrow \mathrm{Li}^{\cdot}_i + V'_{\mathrm{Li}}, \quad (4)$$

$$2\mathrm{OH}^x_{\mathrm{OH}} \Leftrightarrow \mathrm{H_2O}^{\cdot}_{\mathrm{OH}} + \mathrm{OH}'. \quad (5)$$

Equation (4) describes the process of $Li^+$ migration over accessible interstitial sites in the lattice, $V^x_i$. Lithium leaves its crystallographic site $\mathrm{Li}^x_{\mathrm{Li}}$ to form a lithium vacancy $V'_{\mathrm{Li}}$ (the Frenkel defect) and the $\mathrm{Li}^{\cdot}_i$ interstitial site occupied by a lithium ion. Significantly, both the empty interstitial site $V^x_i$ and the one occupied by the lithium ion, $\mathrm{Li}^{\cdot}_i$, are distributed over the "oxygen" planes of the trilayer stacks whose raticular density is one half of that of the "lithium" planes (Fig. 1). This situation is no longer characteristic of the classical Frenkel effect. Equation (5) describes the process of "internal" disproportionation (autoprotolysis) of hydroxide ions. It is typically employed as a basis in treating proton migration in oxygen-containing systems [3, 4, 10–15]. Disproportionation (5) can be a fast enough process only for hydroxide ions capable of rotation, which depends on structural (steric) factors, primarily on rigid bond fixation illustrated by Fig. 1. Besides, Raman and IR spectroscopy did not reveal in LiOH any manifestation of the O–H...O bond, which likewise could initiate reaction (5) [18–20].

The mechanisms of migration characteristic of each type of ion may be considered independently. The self-diffusion activation energies of all the three ions calculated for the temperature region below 650 K as $E_{\mathrm{act}} = \partial(\ln(T\mathcal{D}))/\partial(1/T)$ for crystal–crystal experiments are as follows: for hydrogen—1.7 eV, for lithium—1.34 eV, and for oxygen—2.15 eV for 600–713 K. Biefeld and Johsim [9] studied the electrical conductivity of LiOH whose temperature dependence below 650 K corresponds to an activation energy of 0.85 ± 0.08 eV, and charge carriers are the lithium ions ($E_{\mathrm{act}}$ was calculated by the present author). The mobility of lithium ions, whose temperature dependence corresponds to an activation energy

of ~1.4 ± 0.2 eV, was shown [23] to play a certain role in NMR spectra. We note that one can visually isolate in Fig. 5 three temperature regions for $\mathcal{D}$(Li), with two of them identified by straight lines. The slopes of these straight lines yield 0.73 ± 0.03 and 1.6 ± 0.1 eV for the activation energies. Regrettably, the number of experimental points in all the publications cited above is less than 6–8. Nevertheless, we immediately notice the relatively close values of the self-diffusion coefficients of Li and H. This could be a random coincidence, but the corresponding probability is not more than moderate, if we allow for the fairly broad temperature interval covered (~100 K). Drawing from the available experimental data on the closeness of the self-diffusion rates of $Li^+$ and $H^+$ in LiOH, the present author forwards a hypothesis by which lithium and hydrogen assist one another, as it were, in the self-diffusion process. The simplest version illustrating this idea is visualized in Fig. 8. We see here a fragment of the structure, actually top view on a trilayer stack. The hydroxide ions (denoted by crosses) lie below, and the one identified by a dot, above the lithium ion plane. Interestingly, by all available reports the distance of the proton from the center of the ion in $OH^-$ is smaller (!) than the crystallochemical radius of the oxygen ion. Now because the O–H bonds are directed perpendicular to the plane of the trilayer stack, i.e., to the plane of the figure, protons $H^{(4)}$, $H^{(5)}$, and $H^{(6)}$ are "obscured" by the oxygen cores, and the proton $H^{(3)}$ is projected as a dot on the oxygen core $O^{(3)}$. Transfer of the $Li^{(1)}$ ion to the interstitial site $V_i$ (reaction (4)) facilitates rotation of the $O^{(3)}$–$H^{(3)}$ bond to the left (see figure) and, accordingly, formation of the $O^{(3)}$–$H^{(3)}$...$O^{(4)}$ weak bond required for reaction (5) to proceed. Turning to physical terms, rotation of the O–H bond means transfer of the proton from, say, orbital $p_z$ to another orbital ($p_x$ or $p_y$). The defect thus formed may conventionally be described by the formula $\{H^{(4)}O^{(4)}...H^{(3)} + Li^{(1)}Li^{(2)}O^{(3)}\}$, and it represents a metastable pair of water molecules and lithium oxide. In the stable state, these are products of dehydration of LiOH, whose enthalpy is close to the activation energy of lithium and hydrogen diffusion known for $T < 650$ K. This may be considered as an indirect argument in support of the proposed model involving simultaneous diffusion of lithium and hydrogen ions. Interestingly, hopping of $Li^+$ into an interstitial site is not necessarily an impetus to an elementary diffusion event. As the latter could rather serve "excitation" of the libration of the $O^{(3)}$–$H^{(3)}$ bond, with $Li^{(1)}$ expelled into the interstitial site by the positive pole of the hydroxide ion dipole, i.e., by the proton. It goes without saying that a more careful analysis could reveal a "combined" elementary event, whose action would extend beyond the boundaries of the trilayer stack and turn out more favorable. In particular, formation of such a defect in a quasi-two-dimensional stack creates changes in the charge density which initiates exchange of such defects among stacks, and it is this that would account for the diffusion of lithium and hydrogen in the three-dimensional volume of the crystal.

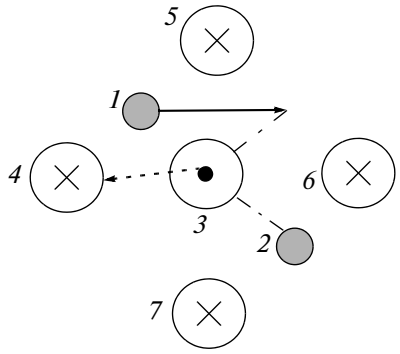


**Fig. 8.** Model of an elementary diffusion event explaining the idea of "mutual assistance" of the lithium ions and protons in the process: (*1*, *2*) lithium ions, (*3*) hydroxide ion whose proton faces us, and (*4*–*7*) hydroxide ions whose protons are directed away from us. Bold arrows specify the motion of the lithium ion (continuous arrow) to the interstitial site on the oxygen plane and rotation of proton *3* (dashed arrow) toward the free oxygen orbital *4*, culminating in formation of a metastable water molecule. The metastable oxide $Li_2O$ is identified by thin dot-dashed lines.

While advancing a somewhat exotic mechanism for diffusion of lithium and hydrogen in lithium hydroxide, the present author does not reject the possibility of "standard" diffusion mechanisms over vacancies of different types; this relates primarily to the diffusion of oxygen. Drawing from the simplest vacancy-based concepts, however, the author has not succeeded in accounting for the diffusion of lithium and hydrogen with comparable rates.

## 4. CONCLUSIONS

Although the subject of the present study—the well known phenomenon of ion self-diffusion, and it is investigated only on one particular material,—lithium hydroxide, the results obtained have significance of a more general nature, which is determined by a number of factors. First, this is a novel approach in experimental studies consisting in simultaneous measurement of self-diffusion of all types of ions ($Li^+$, $H^+$, $O^{2-}$) making up the structure of the material chosen. Second, this is a nonstandard methodology developed particularly for solution of an unconventionally formulated problem, which has permitted us to reduce the effect of poorly controlled factors (impurities, texture, conditions of synthesis and diffusion annealing) and, thus,

to provide a reliable comparison of the mobilities of ions of three types, lithium, oxygen, and hydrogen, Third, it is the main conclusions that can be drawn from the experimental results amassed. They are of practical significance for development of theoretical models describing ion transport in hydrogen- and lithium-containing oxide-type dielectrics. It turned out that the mobilities of lithium and hydrogen are substantially higher than that of oxygen. This implies immediately that hydrogen, while being a part of the hydroxide ion, a lattice building block, migrates independently. The higher mobility of lithium ions compared with that of oxygen ions does not appear strange. At the same time, the fairly close mobilities of the lithium and hydrogen ions is certainly an unexpected finding. It has become a basis of the hypothetical model involving "mutual assistance", as it were, rendered by these ions as they migrate over a layered crystal lattice.

This study has benefited from participation in experiments and discussion of their results of researchers working in three laboratories of the Ioffe Physical-Technical Institute of the Russian Academy of Sciences, engaged in physicochemical studies of isotopes, physics of phase transitions, and dynamics of materials. They are V. B. Ptashnik, A. A. Kabanova, B. S. Nikolaev, E. K. Shalkova, B. Sh. Él'kin, V. M. Egorov, and T. A. Perevalova, to whom the present author expresses his warm and sincere gratitude.

## *APPENDIX*

### *Homomolecular Isotope Exchange as an Additional Method for Investigating Self-Diffusion in Solid LiOH*

The technique employed and the ideology accepted in treating the results of investigation of homomolecular isotope exchange (homoexchange) were developed in considerable detail by Boreskov and Muzykantov [28]. The essence of these experiments consists in investigating relaxation in a purposefully tailored nonequilibrium mixture of isotope forms of oxygen molecules $^{16}O_2$, $^{16}O^{18}O$, and $^{18}O_2$, or hydrogen molecules $H_2$, HD, and $D_2$, under active participation in the process of a solid body, in our particular case, of lithium hydroxide. Under "active participation" one understands here that on the surface of a solid its oxygen ions (or protons) trade their places with the atoms of oxygen (or hydrogen) which have formed in dissociative adsorption of gaseous molecules.

The experimental technique employed in homoexchange did not differ in anything from the one accepted in studies of the gas–crystal heteroexchange (see Subsection 2.4.1).

Homomolecular isotope exchange in the hydrogen–hydroxide system was studied on 0.10–0.25 μm powders (as obtained from mesh size measurements). Following the line developed in [28], we conducted experiments of two types. In one of them, involving bringing in contact powder with composition $A$ with $D_2$ gas, we determined qualitatively the exchange type from the predominant appearance of the $H_2$ peak, which is characteristic of the so-called type-three exchange observed typically in high-efficiency catalysts. In experiments of the second type, the reaction rate was determined quantitatively. In the course of an experiment, one derived the rate of formation of HD molecules in the originally nonequilibrium $H_2 : D_2 = 1 : 1$ mixture at different temperatures and pressures of the gas phase. By the concept outlined in [28], the rate constant of homoexchange $G_3$ for the third type of exchange is equal to that of the heteroexchange reaction, $I_0$, which was considered instrumental to estimate D(H). The temperature dependence of $G_3$ for 7 kPa corresponds to an activation energy of 1.3 eV (Fig. 5). The dependence on gas pressure is weaker than linear, $\sim P(H_2)^{0.8}$. Because these studies do not bear directly on the main goal of the work, we omit here the attendant details.

Homomolecular isotope exchange in the oxygen–hydroxide system was studied on the same 0.10–0.25-μm powders as those employed with hydrogen. The experiments were conducted in the following way. The powder of composition $A$ was brought in contact at 713 K with molecular oxygen (56 at % $^{18}O$) at $\lambda \sim 1$. During the first 30 min one observed the predominant appearance of the $^{16}O^{18}O$ peak, or the so-called exchange of the second type, which is characteristic of relatively less efficient oxygen catalysts [28]. About 3 h later, the isotope composition of the gas reached $\sim 28 \pm 2$ at % $^{18}O$, signaling the onset of the gas–powder isotope equilibrium. This powder was subsequently used in determination at other temperatures of the rate of homoexchange in contact with oxygen of the same isotope composition ($\sim 28 \pm 2$ at % $^{18}O$), but with the nonequilibrium mixture $^{18}O_2 : {}^{18}O^{16}O : {}^{16}O_2 = 0.15 : 0.25 : 0.60$ (to be confronted with 0.08 : 0.40 : 0.52 for the equilibrium ratios of these forms). The homoexchange rate was deduced from the changes observed for the $^{16}O^{18}O$ fraction at temperatures of 560 and 590 K (~24 h), 620 and 650 K (3–4 h), and 680 and 710 K (10–20 min). Specified in parentheses is the approximate sampling times when the $^{16}O^{18}O$ fraction varied from 0.25 to 0.28–0.32 (at equilibrium, the $^{16}O^{18}O$ fraction is 0.40). By the concept forwarded in [28], the rate of homoexchange $G_2$ for the second type is twice the rate of heteroexchange $I_0$. The behavior with temperature of $G_2$ for the pressure of 7 kPa corresponds to the activation energy of 2.3 eV, a figure nearly twice that for hydrogen (Fig. 5).

The pressure dependence of $G_2$ approaches a linear course up to 70 kPa.

## ACKNOWLEDGMENTS

This study was supported by the Presidium of the Russian Academy of Sciences (Program P-03 "Quantum Physics of Condensed Matter").

## REFERENCES

1. I. D. Campbell and C. K. Coogan, J. Chem. Phys. **42** (8), 2738 (1965).
2. D. T. Amm and S. L. Segel, J. Chem. Phys. **80** (10), 4679 (1984).
3. K. D. Kreuer, Chem. Mater. **8**, 610 (1996).
4. F. Freund, H. Wengeler, and R. Martens, J. Chim. Phys. **77** (9), 837 (1980).
5. D. T. Amm, S. L. Segel, and K. R. Jeffrey, Can. J. Phys. **64**, 22 (1986).
6. J. W. Otto and W. B. Holzapfel, J. Phys.: Condens. Matter **7**, 5461 (1995).
7. R. Mörtel and H. D. Lutz, J. Mol. Struct. **648**, 171 (2003).
8. S. Pizzini, J. Appl. Electrochem. **1**, 153 (1971).
9. R. M. Biefeld and R. T. Johsim, J. Electrochem. Soc. **128** (1), 1 (1979).
10. P. M. S. Stephen and A. T. Howe, Solid State Ionics **1**, 461 (1980).
11. K.-H. Haas and U. Schindewolf, Ber. Bunsen-Ges. **87**, 346 (1983).
12. Yu. M. Baĭkov, Élektrokhimiya **28**, 1410 (1982).
13. B. Sh. Él'kin, E. K. Shalkova, and Yu. M. Baĭkov, Izv. Akad. Nauk SSSR, Neorg. Mater. **23** (1), 81 (1987).
14. B. Sh. El'kin, Solid State Ionics **37**, 139 (1990).
15. M. Spaeth, K. D. Kreuer, and Th. Dippel, and J. Maier, Solid State Ionics **97**, 291 (1997).
16. M. Spaeth, K. D. Kreuer, J. Maier, and C. Cramer, J. Solid State Chem. **148**, 169 (1999).
17. Yu. M. Baĭkov and E. K. Shalkova, Kinet. Katal. **21** (6), 1426 (1980).
18. L. S. Itkina, *Hydroxides of Lithium, Rubidium, and Cesium* (Nauka, Moscow, 1979) [in Russian].
19. D. M. Adams, A. G. Chrosbi, and J. Haines, J. Phys. Chem. **96** (20), 8173 (1992).
20. M. Pagliai, M. Iannuzzi, G. Cardini, M. Parrinello, and V. Schettino, ChemPhysChem **7**, 141 (2006).
21. Yu. M. Baĭkov and V. B. Ptashnik, Fiz. Tverd. Tela (Leninngrad) **16** (3), 961 (1974) [Sov. Phys. Solid State **16** (3), 622 (1974].
22. R. T. Johnson, R. M. Biefeld, and I. D. Keck, Mater. Res. Bull. **12** (6), 577 (1977).
23. D. M. Follstaedt and R. M. Biefeld, Phys. Rev. B: Condens. Matter **18** (11), 5928 (1978).
24. B. Sh. Él'kin, E. K. Shalkova, and Yu. M. Baĭkov, Izv. Akad. Nauk SSSR, Neorg. Mater. **23** (1), 86 (1987).
25. A. A. Medvinskii, Yu. M. Baikov, N. N. Bulgakov, and U. F. Stas, React. Kinet. Catal. Lett. **22** (3–4), 362 (1983).
26. A. K. Ivanov-Shits and I. V. Murin, *Solid State Ionics* (St. Petersburg State University, St. Petersburg, 2000).
27. R. Haul, G. Dümbgen, and D. Just, Z. Phys. Chem. (Muenchen) **31**, 309 (1962).
28. V. S. Muzykantov, React. Kinet. Catal. Lett. **35**, 437 (1987).

*Translated by G. Skrebtsov*